© 2022. Published by The Company of Biologists Ltd | Development (2022) 149, dev200190. doi:10.1242/dev.200190

RESEARCH ARTICLE

Drosophila CTP synthase regulates collective cell migration by controlling the polarized endocytic cycle

Pei-Yu Wang[1,2,*], Archan Chakraborty[1,3,*], Hsin-Ju Ma[1], Jhen-Wei Wu[4], Anna C.-C. Jang[4], Wei-Cheng Lin[1,5], Hai-Wei Pi[6,7], Chau-Ting Yeh[7,8], Mei-Ling Cheng[6,7,9,10], Jau-Song Yu[1,5,7,8] and Li-Mei Pai[1,5,7,8,‡]

ABSTRACT

Phosphatidylinositol (PI) 4,5-bisphosphate (PIP_2) is involved in many biological functions. However, the mechanisms of PIP_2 in collective cell migration remain elusive. This study highlights the regulatory role of cytidine triphosphate synthase (CTPsyn) in collective border cell migration through regulating the asymmetrical distribution of PIP_2. We demonstrated that border cell clusters containing mutant CTPsyn cells suppressed migration. CTPsyn was co-enriched with Actin at the leading edge of the *Drosophila* border cell cluster where PIP_2 was enriched, and this enrichment depended on the CTPsyn activity. Genetic interactions of border cell migration were found between CTPsyn mutant and genes in PI biosynthesis. The CTPsyn reduction resulted in loss of the asymmetric activity of endocytosis recycling. Also, genetic interactions were revealed between components of the exocyst complex and CTPsyn mutant, indicating that CTPsyn activity regulates the PIP_2-related asymmetrical exocytosis activity. Furthermore, CTPsyn activity is essential for RTK-polarized distribution in the border cell cluster. We propose a model in which CTPsyn activity is required for the asymmetrical generation of PIP_2 to enrich RTK signaling through endocytic recycling in collective cell migration.

KEY WORDS: CTP synthase, PIP_2, Border cell migration, RTK signaling, *Drosophila*

INTRODUCTION

Cell migration is an important process involved in developmental events and pathologies, such as inflammation and cancer cell metastasis. The migration process is categorized into two types: individual and collective cell migration. Both types of migration involve directed cell migration, implying cell interaction with the environment that includes many mechanisms for sensing guidance signaling and depositing molecules in a polarized manner (Maritzen et al., 2015; Montell et al., 2012; Rørth, 2011). Here, we investigated how cytidine triphosphate synthase (CTPsyn) affected collective cell migration.

Drosophila border cells are used to study collective cell migration *in vivo*. The border cell cluster migrates during *Drosophila* oogenesis and is composed of two polar cells at the center surrounded by six to eight border cells. In the stage 8 egg chamber, the polar cells direct nearby follicle cells to form border cells through activation of JAK/STAT signaling (Montell et al., 2012; Silver and Montell, 2001). In the stage 9 egg chamber, the border cells begin migration from the anterior of the egg chamber to the junction of nurse cells and the oocyte. Once they reach the junction, the border cells migrate to meet the dorsal-anterior follicle cells in the stage 10 egg chamber to participate in micropyle formation, which is the path for sperm entry in fertilization (Prasad et al., 2015) (Fig. 1A). During this process, the extracellular signals are ligands of receptor tyrosine kinase (RTK) which act as guidance cues, such as ligands of epidermal growth factor receptor (EGFR) and PVR (the *Drosophila* homolog of platelet-derived growth factor receptor and vascular endothelial growth factor receptor) (Duchek and Rørth, 2001; Duchek et al., 2001; McDonald et al., 2006). These activated RTKs are restricted to the leading edge of the migratory border cell cluster through endocytic recycling cycles (Assaker et al., 2010; Janssens et al., 2010). The endocytic recycling cycle comes from the PVR signal that acts on Actin polymerization through Rac, which controls Actin as the track for vesicle movement (Ramel et al., 2013; Wan et al., 2013). This leads to amplification of the initial small difference between RTK signaling levels at the front and at the back (Montell et al., 2012; Rørth, 2011; Saadin and Starz-Gaiano, 2016). However, the detailed mechanism of polarized establishment is unclear in collective cell migration.

Phosphoinositol phosphate (PIP) plays important roles in many biological functions from invertebrates to vertebrates, such as cell polarity, cell migration, cell signaling transduction and vesicle trafficking (Schink et al., 2016). PIP is composed of a myo-inositol head group and acyl chain tails. CTPsyn is involved in PIP biosynthesis to produce CTP for forming CDP-diacylglycerol (CDP-DAG) with phosphatidic acid (PA) in *de novo* synthesis (Chang and Carman, 2008). Subsequently, phosphatidylinositol synthase (Pis), an evolutionarily conserved enzyme in PIP biosynthesis, produces phosphatidylinositol (PI), which contains seven derivates that are generated by PIP kinases phosphorylating the 3-, 4-, and 5- groups of the inositol ring individually or in various combinations. Phosphatidylinositol 4-kinase alpha (PI4KIIIα) phosphorylates the 4-group of the inositol ring of PI to form PI4P (Tan and Brill, 2014). PI4P 5-kinase Skittles (Sktl), a phosphatidylinositol 4-phosphate 5-kinase (PIP5K) homolog in *Drosophila*, further phosphorylates the 5-group of inositol rings to

[1]Department of Biochemistry and Molecular Biology, College of Medicine, Chang Gung University, Taoyuan 33302, Taiwan. [2]Research Center for Emerging Viral Infections, College of Medicine, Chang Gung University, Taoyuan 33302, Taiwan. [3]Pharmacology and Cancer Biology, Duke University, Durham, NC 27705, USA. [4]Department of Biotechnology and Bioindustry Sciences, National Cheng Kung University, Tainan City 701, Taiwan. [5]Molecular Medicine Research Center, Chang Gung University, Taoyuan 33302, Taiwan. [6]Department of Biomedical Sciences, College of Medicine, Chang Gung University, Taoyuan 33302, Taiwan. [7]Graduate Institute of Biomedical Sciences, College of Medicine, Chang Gung University, Taoyuan 33302, Taiwan. [8]Liver Research Center, Chang Gung Memorial Hospital, Linkou 333423, Taiwan. [9]Healthy Aging Research Center, Chang Gung University, Taoyuan 33302, Taiwan. [10]Clinical Metabolomics Core Laboratory, Chang Gung Memorial Hospital, Linkou 333423, Taiwan.
*These authors contributed equally to this work

‡Author for correspondence (pai@mail.cgu.edu.tw)

P.-Y.W., 0000-0003-2489-3301; A.C., 0000-0001-9985-0547; W.-C.L., 0000-0003-2970-635X; H.-W.P., 0000-0002-3299-0294; J.-S.Y., 0000-0002-4295-983X; L.-M.P., 0000-0002-1417-6432

Handling Editor: Thomas Lecuit
Received 22 September 2021; Accepted 12 July 2022

Development (2022) 149, dev200190. doi:10.1242/dev.200190

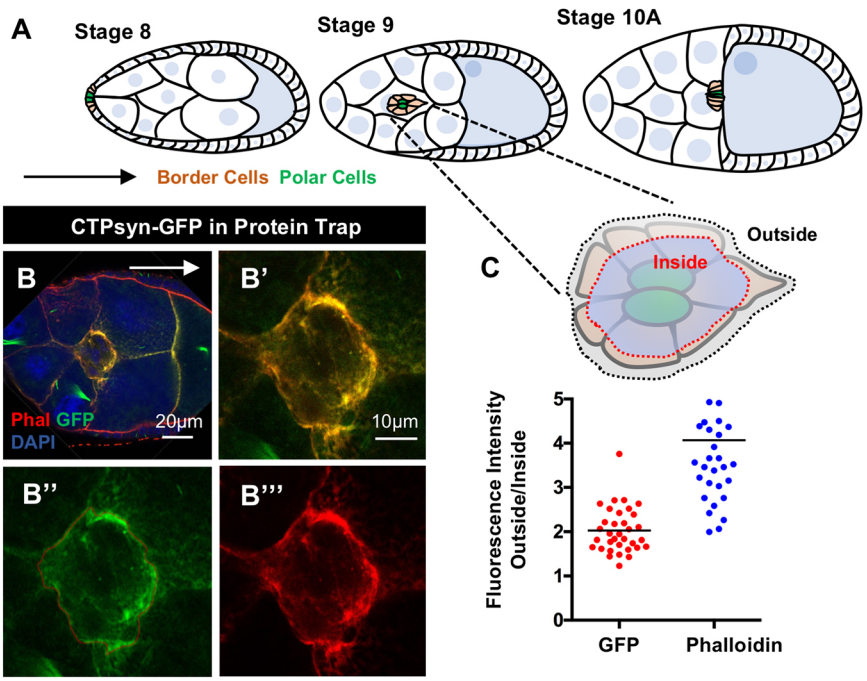

Fig. 1. CTPsyn is enriched at the cell cortex of border cells. (A) A diagram of border cell migration. (B) CTPsyn localization is shown by the expression of GFP-tagged CTPsyn (green) in protein trap and stained with Phalloidin (red). The nucleus is shown by DAPI staining (blue). The magnified border cell cluster from B is shown in B′-B‴. (C) GFP and Actin intensity at the cell cortex (gray area divided by the red area) in border cells were measured in CTPsyn protein trap flies. *n*=34. Quantification shows mean (black lines) and individual data points (red and blue dots).

produce PI 4,5-bisphosphate [PI(4,5)P_2, or PIP_2]. PIP_2 plays a major regulatory role on the cell surface, for example being a precursor of PI(3,4,5)P_3 and an adaptor for membrane and cytosolic protein binding (e.g. N-WASP, PLCδ, Profilin, and RhoGAPs/GEFs). PIP_2 regulates a variety of cellular processes, including endocytosis, exocytosis, cell motility, adhesion and signal transduction (Di Paolo and De Camilli, 2006; Murray et al., 2012). For example, PIP_2/PIP_3 is enriched at the leading edge and directs cell movement of several cell types, including *Dictyostelium* amoebae, mammalian neutrophils and *Drosophila* hemocytes (Funamoto et al., 2002; Kölsch et al., 2007; Lacalle et al., 2007; Rickert et al., 2000; Ridley et al., 2003). CTPsyn reportedly affects the activity of PI synthase in yeast and regulates PIP_2 production in *Drosophila* germline cells (McDonough et al., 1995; Strochlic et al., 2014). However, the role of PIP_2 in collective cell migration remains elusive, and the role of CTPsyn in cell migration is still unknown.

In response to starvation, CTPsyn can assemble into filamentous structures which is well conserved across the species (Aughey et al., 2014; Calise et al., 2014; Carcamo et al., 2011; Ingerson-Mahar et al., 2010). We recently demonstrated that CTPsyn filaments are assembled along a cytokeratin network and histidine-mediated protein methylation promotes its formation in mammalian cancer cells (Chakraborty et al., 2020; Lin et al., 2018). *Drosophila* ovaries express three different isoforms of CTPsyn: isoform A is localized in the nucleus, isoform B is diffused in the cytosol and only isoform C can form the filament (Azzam and Liu, 2013). Based on our previous report, CTPsyn regulates S phase occurrence through its filamentous structure in *Drosophila* ovarian follicle cells, which is positively regulated by the E3 ubiquitin ligase Cbl (Wang et al., 2015). During initial border cell migration, the CTPsyn filamentous structure in anterior follicle cells is disassociated, while the epithelial cell type is transformed into migratory cells by JAK/STAT signaling activation. Therefore, we considered that CTPsyn may play another role in *Drosophila* border cells. Here, we found that CTPsyn is enriched at the outer cortical region of the border cell cluster together with Actin. Depletion of CTPsyn impaired the border cell cluster migration and affected the polarized distribution of PIP_2. Our results suggest that this could alter the PIP_2-involved endocytic recycling pathway and impair the activated RTK-polarized distribution in border cell clusters, which is important for guiding cell migration.

RESULTS

CTPsyn is involved in border cell migration

According to our previous study, CTPsyn filaments are present in every follicle cell of stage 2∼10A egg chambers and are involved in DNA endoreplication during stages 7∼10 (Wang et al., 2015). However, CTPsyn filamentous structures were absent in border cells after cell fate determination by JAK/STAT signaling. Here, we used the CTPsyn protein trap line in which GFP is trapped in-between the first and second exon of isoform C, to investigate the distribution of CTPsyn in border cell clusters (Azzam and Liu, 2013). The distribution of CTPsyn is well colocalized with Actin near the outer cortical region of migrating border cells, and especially at the leading edge (Fig. 1B-C). To investigate whether CTPsyn depletion can affect border cell migration, we expressed CTPsyn RNAi using Slbo-GAL4 in wild-type or $CTPsyn^{d06966}$ mutant background. $CTPsyn^{d06966}$ largely reduces the level of the filament-forming isoform C (Azzam and Liu, 2013). We found that with expression of CTPsyn RNAi in wild-type background, 65% of the border cell clusters migrated to the oocyte border by stage 10, according to the categories mentioned in Fig. 2A,B. However, the complete migratory phenotype further decreased by 32% when CTPsyn RNAi was expressed in the heterozygous $CTPsyn^{d06966}$ null mutant background (Fig. 2B). The enhanced migration defect in the CTPsyn mutant background indicated that it correlated with CTPsyn function (Fig. 2B-F).

Efficiency of CTPsyn RNAi was validated in follicle cells and nurse cells by immunostaining and western blotting, respectively (Fig. S1A-D). In addition, CTPsyn RNAi was driven with c306-GAL4 and Slbo-GAL4 at 29°C instead of 25°C, to increase the RNAi effect. Following this, only 39% and 38% of the border cell clusters, respectively, migrated completely (Fig. S1E-I). c306-GAL4 expresses earlier in border cells and usually leads to stronger

Development (2022) 149, dev200190. doi:10.1242/dev.200190

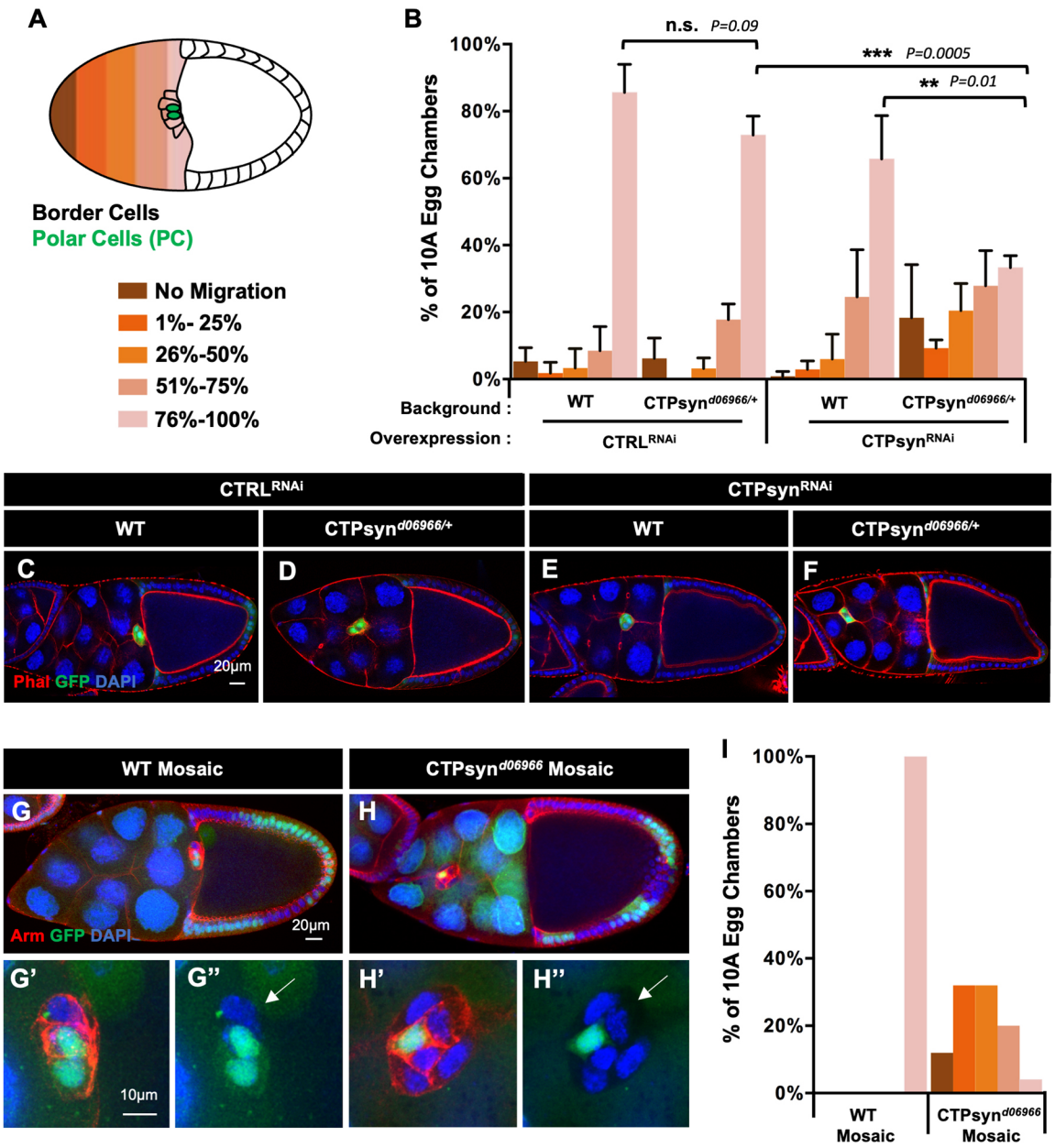

Fig. 2. CTPsyn is involved in regulating border cell migration. (A) Schematic of stage 10 egg chambers showing categorized migration defect of border cell cluster. The extent of migration examined is measured as no migration (dark brown), 1-25% (dark orange), 26%-50% (orange), 51-75% (light orange) and 76-100% (light pink). (B) Border cell cluster migration impeded with CTPsyn reduction. Quantification of the border cell migration in stage 10 egg chambers showing the average from at least three independent experiments. Color scale same as in A (total egg chamber: 91<*n*<120 for each genotype). The results are shown as mean±s.d. (two-tailed unpaired Student's *t*-test). ns, not significant. Crosses were maintained at 25°C for 5 days. (C-F) Representative images of each genotype used in B. GFP (green) expression marks the border cell cluster. Actin boundary and nucleus is stained with Phalloidin (red) and DAPI (blue), respectively. The genotypes are *Slbo-GAL4::UAS-GFP/+;CTRL^{RNAi}/+* (control; C), *Slbo-GAL4::UAS-GFP/+;CTPsyn^{d06966}/CTRL^{RNAi}* (D), *Slbo-GAL4::UAS-GFP/+;CTPsyn^{RNAi}/+* (E), and *Slbo-GAL4::UAS-GFP/+;CTPsyn^{RNAi}/CTPsyn^{d06966}* (F). (G-H″) Border cell clusters showing mosaic wild-type (G) and *CTPsyn^{d06966}* (H) mutant clones. The genotypes are *e22c-GAL4::UAS-FLP/+;Ubi-GFP, FRT80B /FRT80B* (control; G) and *e22c-GAL4::UAS-FLP/+;Ubi-GFP, FRT80B /CTPsyn^{d06966} FRT80B* (H). Magnified images from G and H are shown in G′,G″ and H′,H″, respectively. GFP-negative cells represent mutant clones (shown by arrow in G″ and H″). (I) Quantification of the border cell migration at stage 10 egg chambers in wild-type and CTPsyn^{d06966} mosaic mutant clones, *n*=25. For induction of clones, crosses were maintained at 29°C for 5 days.

phenotypes than Slbo-GAL4. Furthermore, when the efficacy of CTPsyn gene silencing was increased using Dicer, complete border cell cluster migration reduced to 32% (Fig. S1E,J,K). To obtain a loss-of-function phenotype instead of just reduction, we used a mosaic assay to generate the *CTPsyn^{d06966}* mutant allele clone in the border cell cluster. Approximately 70% of mosaic border cell clusters with more than two mutant cells reduced migration to less than 50% (Fig. 2G-I; Fig. S2A-C), and less than 5% of egg chambers with mosaic clones completed the migration. Although, no anterior versus posteriors positional preference was detected for CTPsyn mutant clones (Fig. S2D) at stage 9 during migration, live imaging of migrating border cell clusters containing CTPsyn mutant clones showed disrupted rotation of border cells and reduced migration of the cluster (see Movie 1 for control, Movie 2 for

Development (2022) 149, dev200190. doi:10.1242/dev.200190

CTPsyn mutant). Taken together, these data suggest that CTPsyn is required for border cell cluster migration.

Depletion of CTPsyn alters the distribution of PIP_2 and Actin in border cells

A previous study reported that knockdown of CTPsyn in germline cells reduced the PIP_2 reporter signal in the plasma membrane and decreased membrane integrity (Strochlic et al., 2014). However, the roles of CTPsyn-mediated PIP_2 biosynthesis in border cells has not been investigated. Here, we examined the distribution of PIP_2 by expressing the UAS-PH-PLCδ-GFP reporter, a fusion protein consisting of the PH domain of phospholipase C (PLC) and GFP (Gervais et al., 2008; Varnai et al., 2002). In wild type, the PH-PLCδ-GFP signals were localized between border cell–border cell junctions and border cell–nurse cell interface, and particularly enriched at the tip of the leading edge during entire migratory processes until reaching the oocyte border by stage 10 (Fig. 3A-E′, G,G′). This unique localization in the border cell cluster is consistent with previous reports indicating that PIP_2 is located at the leading edge of human (mammalian) migrating cells and is required for migration function (Czech, 2000). These polarized distributions of PH-PLCδ-GFP signals at the tip of the leading edge were impaired in the CTPsyn-depleted border cell cluster, but the signals of border cell–border cell junctions were not altered (Fig. 3F,F′,H,H′). The ratio of PH-PLCδ-GFP signals between the leading and trailing edge was 2.4-fold in wild type but was reduced to 1.5-fold in CTPsyn-depleted border cell clusters, while the total level of PH-PLCδ-GFP showed no difference (Fig. 3I; Fig. S3A). Depletion of CTPsyn resulted in the loss of enrichment of PIP_2 (GFP-PH^{PLC}) at the leading edge of the border cell cluster, indicating that CTPsyn regulates PIP_2 localization in border cells.

Furthermore, we found that knockdown of CTPsyn in border cell clusters reduced Actin enrichment at the leading edge, as monitored in early stage 9 egg chambers (Fig. 3J-L). Given that PIP_2 is known to promote Actin assembly, reduction of PIP_2 signal at the leading edge caused by CTPsyn depletion could diminish the Actin enrichment (Janmey et al., 2018; Lassing and Lindberg, 1988).

CTPsyn regulates border cell migration through phosphatidylinositide biosynthesis

We then further examined whether CTPsyn regulates border cell migration through PIP_2 production by genetic interaction approaches. Here, we knocked down the genes encoding PIP biosynthesis enzymes (Pis, PI4KIIIα and Sktl, shown in Fig. 4A) in border cells under wild-type or *CTPsyn*^{d06966} heterozygous mutant backgrounds. Knockdown of *pis* by itself did not show migration defects, however in the *CTPsyn*$^{d06966/+}$ background, 58% of stage 10 egg chambers showed border cell migration defects (Fig. 4B-F). Knockdown of *PI4KIIIα* in the wild-type background resulted in 31% of egg chambers with migration defects, which was enhanced in *CTPsyn*$^{d06966/+}$ background by 31%. Although knockdown of *sktl* displayed border cell migration defects, depletion of Sktl did not show genetic interaction with CTPsyn (Fig. 4B,G,H). In humans PI5P can be converted to PIP_2; however, in *Drosophila* this pathway is still unknown (Fig. 4A). These synergistic genetic interactions indicate that CTPsyn cooperates with Pis and PI4KIIIα in PIP biosynthesis to regulate border cell migration.

Altered localization of PIPs by CTPsyn depletion affects endocytic trafficking

PIP_2 is involved in recruiting the correct coat and adaptor proteins during endocytosis, and PI phosphatases like synaptojanin and src-homology 2 containing 5-phosphatase (SHIP2) terminate this recruitment and subsequently PIP_2 is hydrolyzed to PI3P (Wallroth and Haucke, 2018). Therefore, we examined whether PI3P is also affected under CTPsyn depletion conditions. The distribution of PI3P in CTPsyn depletion of border cells was investigated by expressing a UAS-2-FYVE-GFP (2×FYVE) marker, as PI3P serves as a docking site on early endosomes for recruiting specific proteins containing the FYVE zinc-finger domain (Marat and Haucke, 2016). The 2×FYVE was asymmetrically localized at the front of the cluster in wild-type border cells as previously reported, but there were weak signals in cells at the back of the cluster during initial migration (Devergne et al., 2007) (Fig. 5A-A″). In contrast, in the CTPsyn-depleted border cell cluster, 2×FYVE signals lost their asymmetrical distribution and were not enriched in the leading cells (Fig. 5B-B″). The average ratio of 2×FYVE signals between the front and back was 4.3-fold in the wild type but was reduced to 1.2-fold in depletion of the CTPsyn border cell cluster (Fig. 5C). This result indicated that depletion of CTPsyn also resulted in an impaired polarized distribution of PI3P at the leading edge of the border cell cluster, suggesting that trafficking of the early endosome was affected in the border cell cluster.

Rab11 and exocyst components (Sec3, Sec5, Sec15) are reportedly required for border cell migration through their roles in endocytotic recycling trafficking of activated RTKs (Assaker et al., 2010; Wan et al., 2013). Although, under *CTPsyn*$^{d06966/+}$ mutant background, depletion of either Rab11 or Rab7 did not significantly suppress the border cell migration (Fig. S4A), we found that the asymmetric distribution of Rab11 at the leading edge of the border cell cluster was significantly affected, but the total level of Rab11 showed no difference (Fig. S3B) (Assaker et al., 2010; Janssens et al., 2010; Wan et al., 2013) (Fig. 5D-F). In the wild type, Rab11-GFP accumulated at the front of the border cell cluster, and an average of 1.8-fold difference in intensity was measured by comparing the signal at the front and the back of the border cell cluster (Fig. 5F). The intensity difference was reduced to 1.2-fold under depletion of CTPsyn (Fig. 5F). As PI4P plays a role in recruiting Rab11-mediated exocysts, the above data suggests that, following CTPsyn depletion, PI4P distribution in border cell clusters might also be affected (Ketel et al., 2016). In addition, knockdown of *sec3* and *sec15* but not *sec5* in the *CTPsyn*$^{d06966/+}$ mutant background affected border cell migration (Fig. 5G; Fig. S4B). Given that RNAi knockdown of *sec3* and *sec15* did not cause a migration defect, this synergetic genetic interaction between CTPsyn and *sec3*/*sec15* indicate that CTPsyn depletion in border cells might affect the polarized distribution of PIPs, thereby affecting the recycling/endocytic pathways during border cell cluster migration.

CTPsyn depletion affects asymmetric distribution of pTyr in the border cell cluster

The asymmetrical enrichment of activated RTK at the leading edge in the border cell cluster is generated by a polarized endocytic recycling cycle. Cbl, an E3 ligase, is involved in internalizing activated RTKs during border cell migration (Jékely et al., 2005). Knockdown of Cbl in *CTPsyn*$^{d06966/+}$ background showed a synergetic interaction in border cell migration defect phenotypes in 40% of stage 10 egg chambers (Fig. 5G). Thus, we further investigated the distribution of activated RTKs in border cell clusters by immunostaining with an anti-pTyr antibody, which has been validated as a reliable local readout of endogenous RTK activity (Jékely et al., 2005). In wild-type cells, pTyr staining showed restriction in front of the leading

Development (2022) 149, dev200190. doi:10.1242/dev.200190

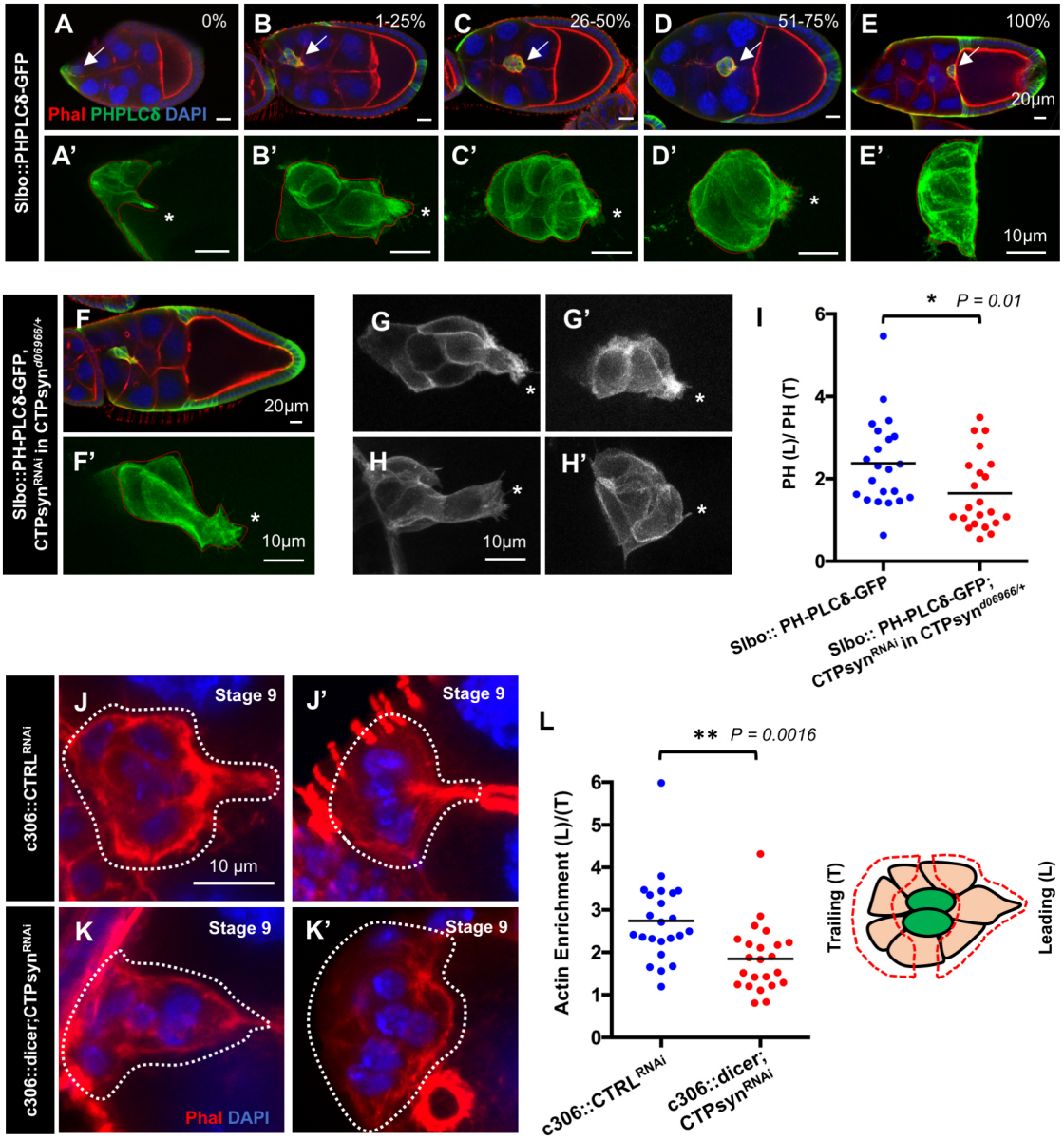

Fig. 3. Depletion of CTPsyn affects PIP_2 asymmetric distribution and Actin enrichment at leading edge. (A-E′) PIP_2 distributions are shown by PH-PLCδ-GFP signals (green). The localization of border cell clusters is indicated as 0% (A), 1-25% (B), 26-50% (C), 51-75% (D) and 100% (E). The arrows indicate border cell clusters. A′-E′ show a magnified view of A-E. Asterisks indicate the protruding leading edge. (F,F′) PH-PLCδ-GFP signal (green) is shown in depleted CTPsyn border cells in stage 10 egg chambers in *Slbo-Gal4::UAS-CTPsyn^{RNAi};UAS-PH-PLC*δ-GFP/CTPsyn^{d06966}. Phalloidin staining is shown in red and DAPI staining is shown in blue. F′ shows a magnified view of F. (G,G′) Two representative images of control border cell cluster in mid stage 9 egg chambers showing enrichment of PH-PLCδ-GFP at the leading edge. (H,H′) Two representative images of border cell cluster with migration defects in stage 10 egg chambers showing reduced enrichment of PH-PLCδ-GFP. (I) The leading-trailing ratio (L/T) of GFP signal was quantified (*n*=23 for each genotype). (J,J′) Two representative images of early stage 9 control egg chambers with Actin enrichment at the leading edge during early events of border cell migration. (K,K′) Representative images of early stage 9 CTPsyn-depleted egg chambers, showing reduction in Actin enrichment. (L) Actin enrichment at the leading edge of border cells was quantified for genotypes *c306-Gal4::CTRL^{RNAi}* and *c306-Gal4::dicer;CTPsyn^{RNAi}*. Experiments were repeated thrice. *n*=23 for each group. Data are mean±s.d. (two-tailed unpaired Student's *t*-test). All crosses were maintained at 29°C.

edge during migration initiation, as previously reported (Fig. 6A). However, depletion of CTPsyn impaired the asymmetrical localization of pTyr signals (Fig. 6B). The pTyr signal ratio between the front and back was 1.5:1 in wild type but was reduced to be 1:1 with depletion of the CTPsyn border cell cluster (Fig. 6I). Furthermore, the enrichment of pTyr signal is also reduced in CTPsyn^{d06966} mosaics (Fig. 6J-K‴). Our results suggest that depletion of CTPsyn abolished the polarized distribution of RTK signaling, indicating that CTPsyn is necessary for regulating the restriction of activated RTKs at the leading edge.

To determine whether CTPsyn is involved in the general sorting of membrane proteins, we visualized adherens junction protein Ecad (also known as Shg) and its partner, Arm, by immunostaining. The patterns of Ecad and Arm were not altered in the border cell cluster with depletion of CTPsyn (Fig. 6C-F; Fig. S2). As the function of PIPs is also required for the polarized architecture of cells, we considered the distribution of cell polarity proteins aPKC and Dlg. The location of aPKC and Dlg was not altered in CTPsyn-depleted border cells or CTPsyn mutant clones (Fig. 6G,H; Fig. S5), suggesting that the failure

Development (2022) 149, dev200190. doi:10.1242/dev.200190

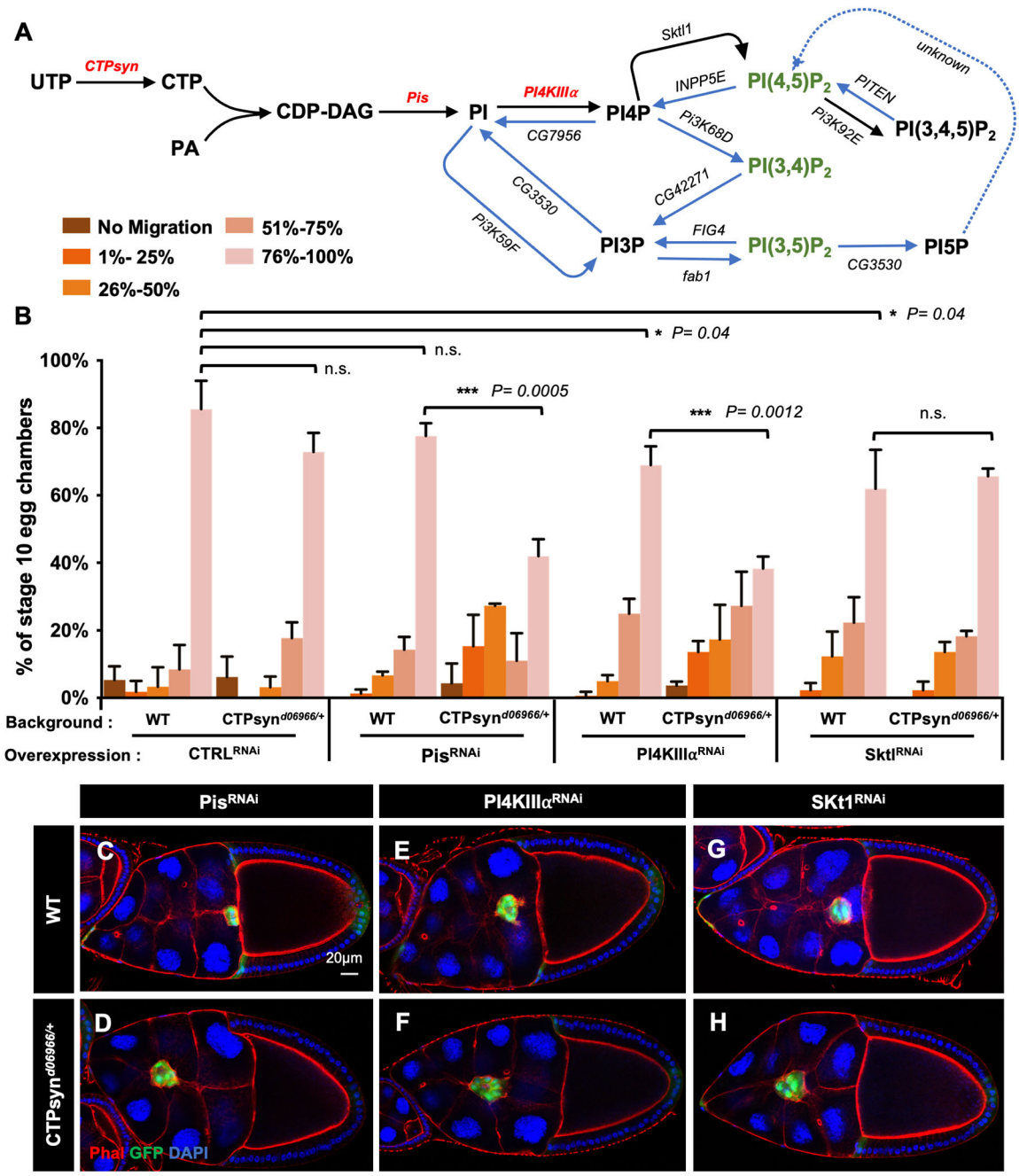

Fig. 4. CTPsyn regulates the border cell migration through its function in PI metabolism. (A) Schematic of the PI metabolism cycle in *Drosophila melanogaster* adapted from KEGG (https://www.genome.jp/kegg/). CTPsyn supplies CTP for CDP-DAG production. Pis catalyzes inositol and CDP-DAG to form PI, which is further phosphorylated by a specific enzyme to form PI derivatives. The three isoforms of phosphoinositides bearing two phosphate groups are shown in green. (B) Quantification of border cell cluster migration defects in stage 10 egg chambers caused by RNAi-mediated knockdown of PI metabolism genes in wild type and *CTPsyn*^{d06966} mutant heterozygous background. The quantification of border cell migration average comes from three independent experiments. Total egg chamber: 75<*n*<154 for each genotype. The results are shown as the mean±s.d. (two-tailed unpaired Student's *t*-test). ns, not significant. (C-H) Representative images of the genotypes quantified in B. The genotypes are *Slbo-Gal4::UAS-GFP/ UAS-Pis*^{RNAi} (C), *Slbo-Gal4:: UAS-GFP/ UAS-Pis*^{RNAi};CTPsyn^{d06966}/+ (D), *Slbo-Gal4::UAS-GFP/UAS-*PI4KIIIα^{RNAi} (E), *Slbo-Gal4:: UAS-GFP/UAS-*PI4KIIIα^{RNAi};CTPsyn^{d06966}/+ (F), *Slbo-Gal4::UAS-GFP/UAS-Skt1*^{RNAi} (G) and *Slbo-Gal4::UAS-GFP/UAS-Skt1*^{RNAi};CTPsyn^{d06966}/+ (H). Border cells are in green, Phalloidin is shown in red and DAPI is shown in blue. *Pis*, *PI4KIIIα* and *Sktl* genes were silenced through RNAi at 29°C.

of restricting activated RTKs did not result from cell polarity disruption.

In summary, CTPsyn regulated the polarized distribution of activated RTK at the leading edge through regulating the polarized endocytic cycle via PIP_2 metabolism in collective cell migration.

DISCUSSION

It is well known that CTPsyn is essential for cell growth by providing building blocks such as DNA, RNA and phospholipids, and the expression of CTPsyn is frequently elevated in cancers (Kizaki et al., 1980; van den Berg et al., 1993; Williams et al., 1978). CTPsyn expression level can regulate the synthesis of

Development (2022) 149, dev200190. doi:10.1242/dev.200190

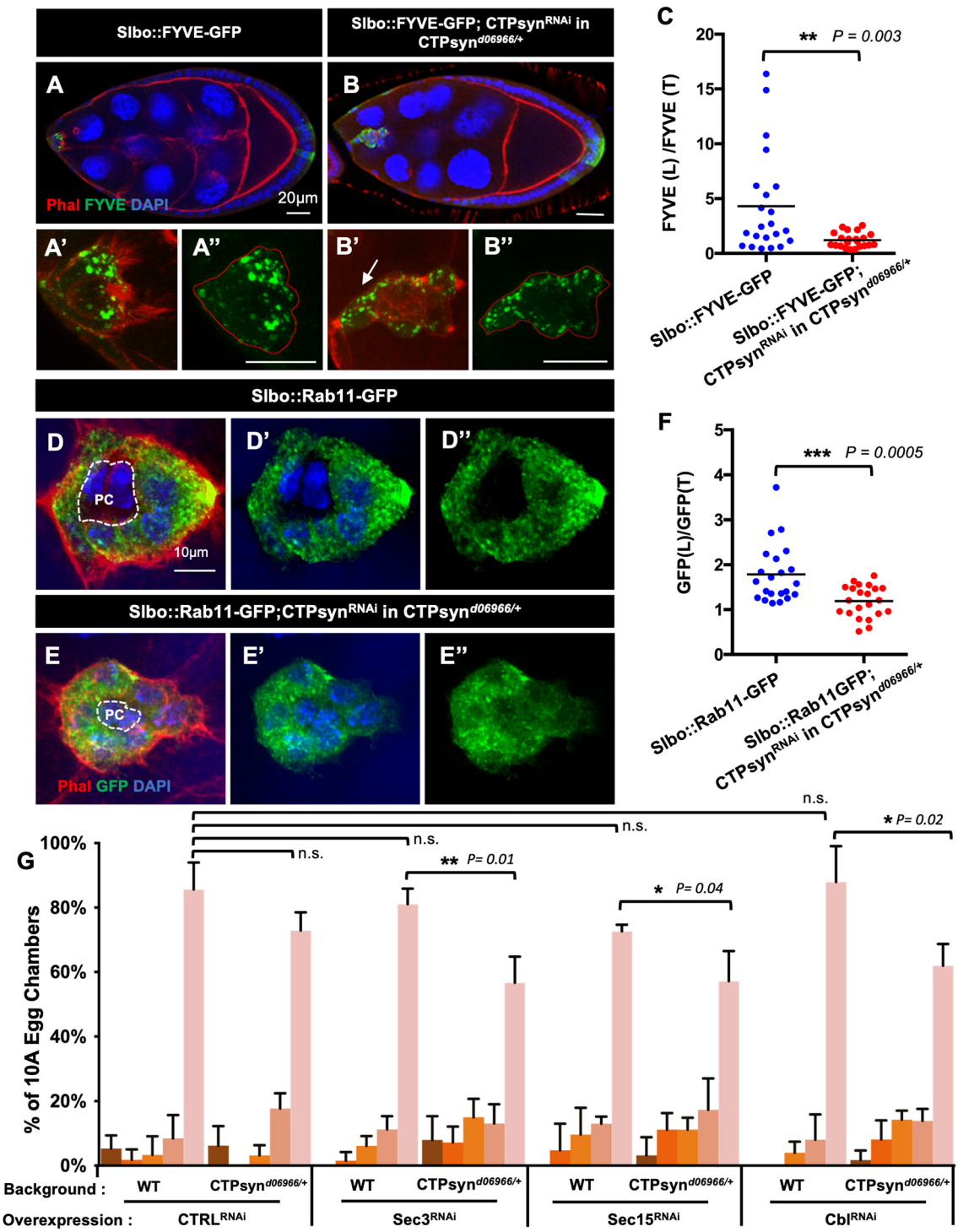

Fig. 5. CTPsyn is involved in endocytic and recycling pathways. (A-B″) Depletion of CTPsyn impaired the asymmetric distribution of the 2×FYVE signal in the border cell cluster. The border cell clusters of the control group (A) and CTPsyn depletion group (B) in stage 9 egg chambers are shown. The 2×FYVE signal is shown in green, and Phalloidin is shown in red. A′,A″ and B′,B″ show magnified views from A and B, respectively. The red line indicates the outline of the border cell cluster (A″,B″). The 2×FYVE signals accumulated at the trailing edge of the CTPsyn-depleted border cell cluster (white arrow). The genotypes are *Slbo-Gal4::UAS-FYVE-GFP*/+ (A) and *Slbo-Gal4::UAS-FYVE-GFP*/+;CTPsyn^{RNAi}/CTPsyn^{d06966} (B). (C) The leading (L)-lagging (T) ratio of GFP signal was quantified for each group (n=22). (D-E″) Depletion of CTPsyn affected Rab11 distribution in border cells. The expression pattern of Rab11-GFP in the wild-type border cell cluster was driven by Slbo-Gal4 (D-D″). The expression pattern of Rab11-GFP is shown in the knockdown CTPsyn border cell cluster under the *CTPsyn*^{d06966} heterozygous mutant background (E-E″). Actin is stained by Phalloidin (red). DAPI is shown in blue. The genotypes are *Slbo-Gal4::UAS-Rab11-GFP*/+ (D) and *Slbo-Gal4::UAS-Rab11-GFP*/+;CTPsyn^{RNAi}/CTPsyn^{d06966} (E). (F) The L-T ratio of GFP signal was quantified for each group (n=22). Crosses were maintained at 29°C. (G) Quantification of border cell cluster migration defects in stage 10 egg chambers caused by RNAi-mediated knockdown of *sec5*, *sec15* and *cbl* at 29°C under wild-type or *CTPsyn*^{d06966} heterozygous mutant background. The total egg chambers: 120<n<180. The averages come from three individual experiments. Data are mean±s.d. (two-tailed unpaired Student's t-test). ns, not significant.

Development (2022) 149, dev200190. doi:10.1242/dev.200190

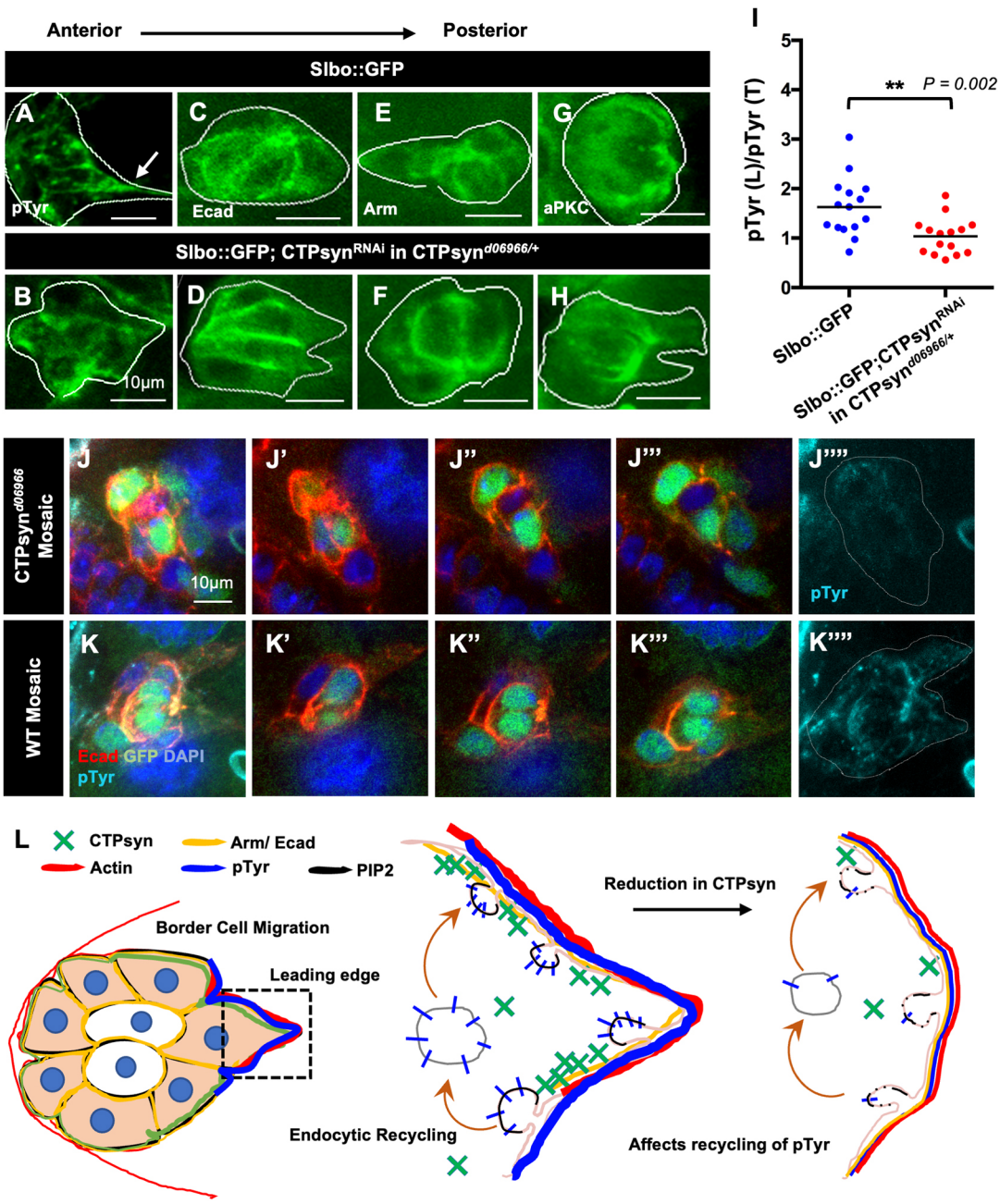

Fig. 6. CTPsyn depletion in border cells disrupts pTyr distribution. (A-H) The control border cell clusters (*Slbo::UAS-GFP/+)* are stained with anti-pTyr (A), Ecad (C), Arm (E) and aPKC (G). The pTyr signal is enriched at the leading edge (arrow in A). The patterns of pTyr (B), Ecad (D) Arm (F) and aPKC (H) are shown in CTPsyn-depleted border cell clusters (*Slbo::UAS-GFP/+;UAS-CTPsyn^{RNAi}/CTPsyn^{d06966}*). The leading edge of the border cell cluster is to the left of the egg chamber. (I) Quantification of the pTyr front (L)-back (T) ratio for stage 9 egg chambers (*n*=15). The results are shown as the mean±s.d. from three independent experiments (two-tailed unpaired Student's *t*-test). (J-K′′′′) Representative images of stage 10 egg chambers with CTPsyn mutant (J-J′′′) and wild type (K-K′′′) mosaic clones. Egg chambers were immunostained with Ecad antibody (red), pTyr antibody (cyan) and DAPI (blue). Clones were induced at 29°C. GFP-negative cells represent the clones. *Z*-sections for border cell clusters are shown in J′-J′′′ and K′-K′′′. Merged *z*-stack image of the pTyr staining of border cell cluster (J′′′′-K′′′′). (L) The model shows the regulatory machinery of CTPsyn in endocytic recycling. CTPsyn depletion in border cell clusters reduces PIP_2 enrichment at the leading edge thereby affecting the RTK signaling (pTyr distribution) and reorganization of Actin networks for cell migration.

CDP-DAG, which is required for the production of phosphoinositides (McDonough et al., 1995). Here, we reveal a role for CTPsyn in collective cell migration through regulation of the asymmetrical distribution of PIP_2 at the leading edge of migrating border cell cluster, suggesting that CTPsyn might have additional roles in tumorigenesis (Fig. 6L). PIP_2 enrichment at the leading edge is essential for directing migration in a single cell (Czech, 2000). PIP_2 is spatially controlled by the activities of metabolized kinases such as phosphoinositide 4-kinase (PI4K) and PIP5K (Clayton et al., 2013; van den Bout and Divecha, 2009). Our results also showed that during collective cell migration, PIP_2 is enriched at the leading edge (Fig. 3). Knockdown of PIP_2 biosynthesis enzymes in the CTPsyn mutant background further suppressed the border cell migration, supporting the idea of PIP_2

Development (2022) 149, dev200190. doi:10.1242/dev.200190

regulation by CTPsyn (Fig. 4). This finding raised an interesting question regarding how a biosynthesis enzyme regulates the spatial distribution of phospholipids. Purine biosynthetic enzymes are compartmentalized at the leading edge in motile renal cell carcinoma (Wolfe et al., 2019). Intriguingly, we found that CTPsyn is also enriched at the cortex of border cell clusters, suggesting a spatial proximity of PI biosynthesis and asymmetrical enrichment of PIP_2 (Fig. 1). One possible explanation for our results is that local high levels of PIs generated by enrichment of CTPsyn is essential for subsequent functioning of phosphoinositide-metabolizing kinases that are also spatiotemporally distributed; however, this hypothesis needs further experiments to verify. Interestingly, live images showed an impairment in mutant CTPsyn border cell rotation during migration at stage 9, indicating the coordination between border cells was disrupted. However, the molecular mechanism of CTPsyn in coordinating border cell rotation needs further investigation.

In epithelial cells, PIP_2 is enriched in the microdomain of the plasma membrane (PM) named the lipid raft, which is characterized by cholesterol enrichment and resistance to Triton X-100 (Johnson et al., 2008; Munro, 2003; Wang and Richards, 2012). This enrichment of PIP_2 on the PM promotes the localization of EGFR in the lipid raft microdomain, which may upregulate PI3K signaling to activate Rac/Cdc42 for Actin polymerization (Abd Halim et al., 2015). PIP_2 is also known to regulate Actin dynamics through interactions with Actin associated proteins (Janmey et al., 2018). Our results showed that depletion of CTPsyn resulted in loss of PIP_2 and Actin enrichment at the leading edge (Fig. 3), indicating that CTPsyn may control border cell migration through regulation of Actin dynamics by the levels of PIP_2. Furthermore, loss of function of CTPsyn in the border cell cluster abolished the pTyr signaling enrichment in the leading edge (Fig. 6B,I-K‴), suggesting that CTPsyn may be required for the formation of raft microdomains of the PM for enriching activated RTKs through the promotion of PIP_2 production. Recently, a rapid dynamic for PIP_2 turnover by PLC and PI4 kinase pathways was discovered in the raft microdomain (Myeong et al., 2021), suggesting that the CTPsyn-mediated biosynthesis of PIP_2 might be crucial for raft domain formation and signaling.

During collective border cell migration, spatial restriction of RTK at the leading edge is maintained by a positive-feedback loop through RTK downstream Rac signaling, which induces polarized distribution of recycling endosome and exocyst, involving Cbl, Rab5, Rab11 and exocyst components (Assaker et al., 2010; Jékely et al., 2005; Wan et al., 2013). The migratory defect of the CTPsyn-depleted border cell cluster was enhanced by interfering with the activity of Cbl and exocyst components (Fig. 5G), suggesting that CTPsyn function is involved in the endocytic recycling cycle to promote directional migration. Furthermore, the polarized distribution of Rab11-GFP and FYVE signals was also abolished in the CTPsyn-depleted border cell cluster (Fig. 5A-F). As asymmetric distribution of RTK was significantly reduced with CTPsyn depletion (Fig. 6B,I-K‴), it is possible that RTK-regulated high levels of recycling vesicles and asymmetrically distributed exocyst were also disturbed. Alternatively, PIP_2 at the PM is required for nucleation of endocytic clathrin-coated pits, and $PI(3,4)P_2$ is the intermediate for the conversion to the PI3P-containing endosome (Posor et al., 2013). Thus, asymmetric PIP_2 enrichment may regulate the asymmetric distribution of endosomal PI3P through endocytosis. Furthermore, the conversion of PI3P to PI4P by MTM1 and PI4KIIα is required for exocyst-dependent endosomal exocytosis due to the binding of PI4P to Rab11 (Ketel et al., 2016; Wallroth and Haucke, 2018). These studies in mammals support our finding that CTPsyn depletion disrupted the asymmetric distribution of Rab11 and PI3P, which may be through the loss of PIP_2 asymmetrical distribution. However, the possibility that CTPsyn might regulate polarized trafficking is not excluded from our study. In summary, we provide here the link between CTPsyn function and PIP_2 production in asymmetrical endocytic and recycling activity during collective cell migration. This may lead us to investigate further the roles of CTPsyn in cancer metastasis and find alternative therapeutic treatments.

MATERALS AND METHODS

Fly stocks

All flies were maintained at 25°C. The following fly lines from Bloomington *Drosophila* Stock Center (BDSC) were used: wild type (Oregon-R), *UAS-PHPLCδ-GFP*, *UAS-GFP-myc-2×FYVE* and *UAS-Sktl^{RNAi}* (TRIP line JF02796). The following fly lines from the Vienna *Drosophila* Resource Center (VDRC) were used: *CTRL^{GD60000}* (CTRL^{RNAi}), *CTPsyn^{GD12759}*, *CTPsyn^{GD12762}*, *PI4KIIIα^{GD15993}*, *Pis^{GD11852}*, *Cbl^{GD22335}*, *Sec3^{GD35806}*, *Sec5^{GD28873}* and *Sec15^{GD35161}*. To drive expression in border cells, *Slbo-GAL4*, *c306-GAL4* and *e22c-GAL4* was used. To drive expression in germ cells *nanos-GAL4* was used. CTPsyn mutant stock (*UAS-CD8::GFP*, *CTPsyn^{d06966}/TM3Ser)* was obtained from BDSC. Wild type (*e22cFLP/+;Ubi-GFP FRT80B/FRT80B*) and mutant mosaic clones (*e22cFLP/+; Ubi-GFP FRT80B/CTPsyn^{d06966}, FRT80B*) were generated using Flp-FRT method. To induce clones, flies were incubated at 29°C. GFP-CTP synthase (CA06746 and CA07332) protein traps were from Ji-Long Liu (Shanghai Tech University, Shanghai, China). For genetic interaction experiments, all crosses were maintained at 29°C unless otherwise mentioned.

Immunostaining

Ovary dissection was performed in Schneider's medium within 5 min and then fixed in 4% paraformaldehyde for 20 min. After washes in PBT (0.3% Triton X-100 in PBS), ovaries were stained with primary antibodies overnight at 4°C. The primary antibodies used for immunostaining included: rabbit anti-CTPsyn (1:300; y-88, sc-134457; Santa Cruz Biotechnology), mouse anti-Ecad [1:50; Developmental Studies Hybridoma Bank (DSHB)], mouse anti-arm (1:50; 7A1; DSHB), mouse anti-phosphotyrosine (1:200; Millipore), rabbit anti-PKCζ (1:200; C-20; Santa Cruz Biotechnology) and mouse anti-Dlg (1:50; 4F3; DSHB). Secondary antibodies included Alexa Fluor 488 or 546 anti-mouse/rabbit/rat antibodies [1:1000; A11001 (anti-mouse), A11008 (anti-rabbit), A11030 (anti-mouse), A11035 (anti-rabbit) and A21050 (anti-mouse); Thermo Fisher Scientific]. To visualize DNA, we added 0.5 mg/ml DAPI (Sigma-Aldrich) for 5 min at room temperature. To visualize Actin, we used Phalloidin (1:100; Molecular Probes).

Analysis of border cell migration

Stage 10 egg chambers were selected, and the position of border cell clusters was analyzed. We defined stage 10 as when the oocyte spanned the posterior half of the egg chamber. As an index for migration, these stage 10 egg chambers were categorized based on the location of the border cell cluster as depicted in Fig. 2A.

Quantification of fluorescence signals

Images from fixed tissues were acquired using a ZEISS LSM 780 inverted confocal microscope. The quantification methods are similar to those previously described (Zhang et al., 2011). For measurement of the front/back (leading/lagging) ratios, an area around the leading edge of the cluster but excluding polar cells (labeled by anti-FasIII antibodies; 1:20, 7G10, DSHB) was chosen as the front region, and an area including the lagging end but excluding polar cells was chosen as the back region. Fluorescence intensity and area were measured using Fiji software for each region. The graphs were plotted with Prism 6. For experimental data, a Student's two-tailed unpaired *t*-test was used for the analysis.

Egg chamber *ex vivo* culture for time-lapse image

The time-lapse image was performed as previously described (Chang et al., 2018). In brief, female flies were dissected in S2 live media which comprised S2 Cell medium, fetal bovine serum (Gibco), insulin (Sigma-Aldrich) and female fly extract. Egg chambers were cultured in ibidi glass-bottomed dishes after dissection. The images were taken every 5 min using a Zeiss Observer D1 microscope. All live images were processed by Axio Vision SE64Rel.4.8.2 software (Media Cybernetics) and the NIS-Elements AR Analysis 4.50.00 64-bit software (Nikon).

Acknowledgements

We are grateful to the Microscopy Center of Chang Gung University, for assistance with image capture. We thank Mark A. Peifer and Robert J. Duronio for critical comments on the manuscript. We also thank the Fly Core in Taiwan, the DSHB, the BDSC and VDRC for providing reagents.

Competing interests

The authors declare no competing or financial interests.

Author contributions

Conceptualization: P.-Y.W., A.C., C.-T.Y., J.-S.Y., L.-M.P.; Methodology: P.-Y.W., A.C.; Validation: P.-Y.W., A.C., H.-J.M.; Formal analysis: P.-Y.W., A.C., H.-J.M., W.-C.L.; Investigation: P.-Y.W., A.C., H.-J.M., J.-W.W., A.C.-C.J., W.-C.L., H.-W.P., M.-L.C.; Data curation: L.-M.P.; Writing - original draft: P.-Y.W., A.C., L.-M.P.; Visualization: P.-Y.W., A.C.; Supervision: L.-M.P.; Project administration: L.-M.P.; Funding acquisition: L.-M.P.

Funding

This work was funded by the Ministry of Science and Technology, Taiwan (MOST 108-2311-B-182-004-MY3 to L.-M.P.), and the Chang Gung Memorial Hospital, Taiwan (CMRPD1I0011-3 to L.-M.P.).

Peer review history

The peer review history is available online at https://journals.biologists.com/dev/article-lookup/doi/10.1242/dev.200190.reviewer-comments.pdf.

References

Abd Halim, K. B., Koldsø, H. and Sansom, M. S. P. (2015). Interactions of the EGFR juxtamembrane domain with PIP2-containing lipid bilayers: insights from multiscale molecular dynamics simulations. *Biochim. Biophys. Acta* **1850**, 1017-1025. doi:10.1016/j.bbagen.2014.09.006

Assaker, G., Ramel, D., Wculek, S. K., González-Gaitán, M. and Emery, G. (2010). Spatial restriction of receptor tyrosine kinase activity through a polarized endocytic cycle controls border cell migration. *Proc. Natl. Acad. Sci. USA.* **107**, 22558-22563. doi:10.1073/pnas.1010795108

Aughey, G. N., Grice, S. J., Shen, Q.-J., Xu, Y., Chang, C.-C., Azzam, G., Wang, P.-Y., Freeman-Mills, L., Pai, L.-M., Sung, L.-Y. et al. (2014). Nucleotide synthesis is regulated by cytoophidium formation during neurodevelopment and adaptive metabolism. *Biol. Open* **3**, 1045-1056. doi:10.1242/bio.201410165

Azzam, G. and Liu, J.-L. (2013). Only one isoform of Drosophila melanogaster CTP synthase forms the cytoophidium. *PLoS Genet.* **9**, e1003256. doi:10.1371/journal.pgen.1003256

Calise, S. J., Carcamo, W. C., Krueger, C., Yin, J. D., Purich, D. L. and Chan, E. K. L. (2014). Glutamine deprivation initiates reversible assembly of mammalian rods and rings. *Cell. Mol. Life Sci.* **71**, 2963-2973. doi:10.1007/s00018-014-1567-6

Carcamo, W. C., Satoh, M., Kasahara, H., Terada, N., Hamazaki, T., Chan, J. Y. F., Yao, B., Tamayo, S., Covini, G., von Muhlen, C. A. et al. (2011). Induction of cytoplasmic rods and rings structures by inhibition of the CTP and GTP synthetic pathway in mammalian cells. *PLoS ONE* **6**, e29690. doi:10.1371/journal.pone.0029690

Chakraborty, A., Lin, W.-C., Lin, Y.-T., Huang, K.-J., Wang, P.-Y., Chang, Y.-F., Wang, H.-I., Ma, K.-T., Wang, C.-Y., Huang, X.-R. et al. (2020). SNAP29 mediates the assembly of histidine-induced CTP synthase filaments in proximity to the cytokeratin network. *J. Cell Sci.* **133**, jcs240200. doi:10.1242/jcs.240200

Chang, Y.-F. and Carman, G. M. (2008). CTP synthetase and its role in phospholipid synthesis in the yeast Saccharomyces cerevisiae. *Prog. Lipid Res.* **47**, 333-339. doi:10.1016/j.plipres.2008.03.004

Chang, Y.-C., Wu, J.-W., Hsieh, Y.-C., Huang, T.-H., Liao, Z.-M., Huang, Y.-S., Mondo, J. A., Montell, D. and Jang, A. C.-C. (2018). Rap1 negatively regulates the Hippo pathway to polarize directional protrusions in collective cell migration. *Cell Rep.* **22**, 2160-2175. doi:10.1016/j.celrep.2018.01.080

Clayton, E. L., Minogue, S. and Waugh, M. G. (2013). Mammalian phosphatidylinositol 4-kinases as modulators of membrane trafficking and lipid signaling networks. *Prog. Lipid Res.* **52**, 294-304. doi:10.1016/j.plipres.2013.04.002

Czech, M. P. (2000). PIP2 and PIP3: complex roles at the cell surface. *Cell* **100**, 603-606. doi:10.1016/S0092-8674(00)80696-0

Devergne, O., Ghiglione, C. and Noselli, S. (2007). The endocytic control of JAK/STAT signalling in Drosophila. *J. Cell Sci.* **120**, 3457-3464. doi:10.1242/jcs.005926

Di Paolo, G. and De Camilli, P. (2006). Phosphoinositides in cell regulation and membrane dynamics. *Nature* **443**, 651-657. doi:10.1038/nature05185

Duchek, P. and Rørth, P. (2001). Guidance of cell migration by EGF receptor signaling during Drosophila oogenesis. *Science* **291**, 131-133. doi:10.1126/science.291.5501.131

Duchek, P., Somogyi, K., Jékely, G., Beccari, S. and Rørth, P. (2001). Guidance of cell migration by the Drosophila PDGF/VEGF receptor. *Cell* **107**, 17-26. doi:10.1016/S0092-8674(01)00502-5

Funamoto, S., Meili, R., Lee, S., Parry, L. and Firtel, R. A. (2002). Spatial and temporal regulation of 3-phosphoinositides by PI 3-kinase and PTEN mediates chemotaxis. *Cell* **109**, 611-623. doi:10.1016/S0092-8674(02)00755-9

Gervais, L., Claret, S., Januschke, J., Roth, S. and Guichet, A. (2008). PIP5K-dependent production of PIP2 sustains microtubule organization to establish polarized transport in the Drosophila oocyte. *Development* **135**, 3829-3838. doi:10.1242/dev.029009

Ingerson-Mahar, M., Briegel, A., Werner, J. N., Jensen, G. J. and Gitai, Z. (2010). The metabolic enzyme CTP synthase forms cytoskeletal filaments. *Nat. Cell Biol.* **12**, 739-746. doi:10.1038/ncb2087

Janmey, P. A., Bucki, R. and Radhakrishnan, R. (2018). Regulation of actin assembly by PI(4,5)P2 and other inositol phospholipids: an update on possible mechanisms. *Biochem. Biophys. Res. Commun.* **506**, 307-314. doi:10.1016/j.bbrc.2018.07.155

Janssens, K., Sung, H.-H. and Rørth, P. (2010). Direct detection of guidance receptor activity during border cell migration. *Proc. Natl. Acad. Sci. USA* **107**, 7323-7328. doi:10.1073/pnas.0915075107

Jékely, G., Sung, H.-H., Luque, C. M. and Rørth, P. (2005). Regulators of endocytosis maintain localized receptor tyrosine kinase signaling in guided migration. *Dev. Cell* **9**, 197-207. doi:10.1016/j.devcel.2005.06.004

Johnson, C. M., Chichili, G. R. and Rodgers, W. (2008). Compartmentalization of phosphatidylinositol 4,5-bisphosphate signaling evidenced using targeted phosphatases. *J. Biol. Chem.* **283**, 29920-29928. doi:10.1074/jbc.M805921200

Ketel, K., Krauss, M., Nicot, A.-S., Puchkov, D., Wieffer, M., Müller, R., Subramanian, D., Schultz, C., Laporte, J. and Haucke, V. (2016). A phosphoinositide conversion mechanism for exit from endosomes. *Nature* **529**, 408-412. doi:10.1038/nature16516

Kizaki, H., Williams, J. C., Morris, H. P. and Weber, G. (1980). Increased cytidine 5'-triphosphate synthetase activity in rat and human tumors. *Cancer Res.* **40**, 3921-3927.

Kölsch, V., Seher, T., Fernandez-Ballester, G. J., Serrano, L. and Leptin, M. (2007). Control of Drosophila gastrulation by apical localization of adherens junctions and RhoGEF2. *Science* **315**, 384-386. doi:10.1126/science.1134833

Lacalle, R. A., Peregil, R. M., Albar, J. P., Merino, E., Martínez, A. C., Mérida, I. and Mañes, S. (2007). Type I phosphatidylinositol 4-phosphate 5-kinase controls neutrophil polarity and directional movement. *J. Cell Biol.* **179**, 1539-1553. doi:10.1083/jcb.200705044

Lassing, I. and Lindberg, U. (1988). Specificity of the interaction between phosphatidylinositol 4,5-bisphosphate and the profilin:actin complex. *J. Cell. Biochem.* **37**, 255-267. doi:10.1002/jcb.240370302

Lin, W.-C., Chakraborty, A., Huang, S.-C., Wang, P.-Y., Hsieh, Y.-J., Chien, K.-Y., Lee, Y.-H., Chang, C.-C., Tang, H.-Y., Lin, Y.-T. et al. (2018). Histidine-dependent protein methylation is required for compartmentalization of CTP synthase. *Cell Rep.* **24**, 2733-2745.e37. doi:10.1016/j.celrep.2018.08.007

Marat, A. L. and Haucke, V. (2016). Phosphatidylinositol 3-phosphates-at the interface between cell signalling and membrane traffic. *EMBO J.* **35**, 561-579. doi:10.15252/embj.201593564

Maritzen, T., Schachtner, H. and Legler, D. F. (2015). On the move: endocytic trafficking in cell migration. *Cell. Mol. Life Sci.* **72**, 2119-2134. doi:10.1007/s00018-015-1855-9

McDonald, J. A., Pinheiro, E. M., Kadlec, L., Schupbach, T. and Montell, D. J. (2006). Multiple EGFR ligands participate in guiding migrating border cells. *Dev. Biol.* **296**, 94-103. doi:10.1016/j.ydbio.2006.04.438

McDonough, V. M., Buxeda, R. J., Bruno, M. E. C., Ozier-Kalogeropoulos, O., Adeline, M.-T., McMaster, C. R., Bell, R. M. and Carman, G. M. (1995). Regulation of phospholipid biosynthesis in Saccharomyces cerevisiae by CTP. *J. Biol. Chem.* **270**, 18774-18780. doi:10.1074/jbc.270.32.18774

Montell, D. J., Yoon, W. H. and Starz-Gaiano, M. (2012). Group choreography: mechanisms orchestrating the collective movement of border cells. *Nat. Rev. Mol. Cell Biol.* **13**, 631-645. doi:10.1038/nrm3433

Munro, S. (2003). Lipid rafts: elusive or illusive? *Cell* **115**, 377-388. doi:10.1016/S0092-8674(03)00882-1

Murray, M. J., Ng, M. M., Fraval, H., Tan, J., Liu, W., Smallhorn, M., Brill, J. A., Field, S. J. and Saint, R. (2012). Regulation of Drosophila mesoderm migration

by phosphoinositides and the PH domain of the Rho GTP exchange factor Pebble. *Dev. Biol.* **372**, 17-27. doi:10.1016/j.ydbio.2012.09.008

Myeong, J., Park, C.-G., Suh, B.-C. and Hille, B. (2021). Compartmentalization of phosphatidylinositol 4,5-bisphosphate metabolism into plasma membrane liquid-ordered/raft domains. *Proc. Natl. Acad. Sci. USA* **118**, e2025343118. doi:10.1073/pnas.2025343118

Posor, Y., Eichhorn-Gruenig, M., Puchkov, D., Schöneberg, J., Ullrich, A., Lampe, A., Müller, R., Zarbakhsh, S., Gulluni, F., Hirsch, E. et al. (2013). Spatiotemporal control of endocytosis by phosphatidylinositol-3,4-bisphosphate. *Nature* **499**, 233-237. doi:10.1038/nature12360

Prasad, M., Wang, X., He, L., Cai, D. and Montell, D. J. (2015). Border cell migration: a model system for live imaging and genetic analysis of collective cell movement. *Methods Mol. Biol.* **1328**, 89-97. doi:10.1007/978-1-4939-2851-4_6

Ramel, D., Wang, X., Laflamme, C., Montell, D. J. and Emery, G. (2013). Rab11 regulates cell-cell communication during collective cell movements. *Nat. Cell Biol.* **15**, 317-324. doi:10.1038/ncb2681

Rickert, P., Weiner, O. D., Wang, F., Bourne, H. R. and Servant, G. (2000). Leukocytes navigate by compass: roles of PI3Kgamma and its lipid products. *Trends Cell Biol.* **10**, 466-473. doi:10.1016/S0962-8924(00)01841-9

Ridley, A. J., Schwartz, M. A., Burridge, K., Firtel, R. A., Ginsberg, M. H., Borisy, G., Parsons, J. T. and Horwitz, A. R. (2003). Cell migration: integrating signals from front to back. *Science* **302**, 1704-1709. doi:10.1126/science.1092053

Rørth, P. (2011). Whence directionality: guidance mechanisms in solitary and collective cell migration. *Dev. Cell* **20**, 9-18. doi:10.1016/j.devcel.2010.12.014

Saadin, A. and Starz-Gaiano, M. (2016). Circuitous genetic regulation governs a straightforward cell migration. *Trends Genet.* **32**, 660-673. doi:10.1016/j.tig.2016.08.001

Schink, K. O., Tan, K.-W. and Stenmark, H. (2016). Phosphoinositides in control of membrane dynamics. *Annu. Rev. Cell Dev. Biol.* **32**, 143-171. doi:10.1146/annurev-cellbio-111315-125349

Silver, D. L. and Montell, D. J. (2001). Paracrine signaling through the JAK/STAT pathway activates invasive behavior of ovarian epithelial cells in Drosophila. *Cell* **107**, 831-841. doi:10.1016/S0092-8674(01)00607-9

Strochlic, T. I., Stavrides, K. P., Thomas, S. V., Nicolas, E., O'Reilly, A. M. and Peterson, J. R. (2014). Ack kinase regulates CTP synthase filaments during Drosophila oogenesis. *EMBO Rep.* **15**, 1184-1191. doi:10.15252/embr.201438688

Tan, J. and Brill, J. A. (2014). Cinderella story: PI4P goes from precursor to key signaling molecule. *Crit. Rev. Biochem. Mol. Biol.* **49**, 33-58. doi:10.3109/10409238.2013.853024

van den Berg, A. A., van Lenthe, H., Busch, S., de Korte, D., Roos, D., van Kuilenburg, A. B. and van Gennip, A. H. (1993). Evidence for transformation-related increase in CTP synthetase activity in situ in human lymphoblastic leukemia. *Eur. J. Biochem.* **216**, 161-167. doi:10.1111/j.1432-1033.1993.tb18128.x

van den Bout, I. and Divecha, N. (2009). PIP5K-driven PtdIns(4,5)P2 synthesis: regulation and cellular functions. *J. Cell Sci.* **122**, 3837-3850. doi:10.1242/jcs.056127

Varnai, P., Lin, X., Lee, S. B., Tuymetova, G., Bondeva, T., Spät, A., Rhee, S. G., Hajnóczky, G. and Balla, T. (2002). Inositol lipid binding and membrane localization of isolated pleckstrin homology (PH) domains. Studies on the PH domains of phospholipase C delta 1 and p130. *J. Biol. Chem.* **277**, 27412-27422. doi:10.1074/jbc.M109672200

Wallroth, A. and Haucke, V. (2018). Phosphoinositide conversion in endocytosis and the endolysosomal system. *J. Biol. Chem.* **293**, 1526-1535. doi:10.1074/jbc.R117.000629

Wan, P., Wang, D., Luo, J., Chu, D., Wang, H., Zhang, L. and Chen, J. (2013). Guidance receptor promotes the asymmetric distribution of exocyst and recycling endosome during collective cell migration. *Development* **140**, 4797-4806. doi:10.1242/dev.094979

Wang, J. and Richards, D. A. (2012). Segregation of PIP2 and PIP3 into distinct nanoscale regions within the plasma membrane. *Biol. Open* **1**, 857-862. doi:10.1242/bio.20122071

Wang, P.-Y., Lin, W.-C., Tsai, Y.-C., Cheng, M.-L., Lin, Y.-H., Tseng, S.-H., Chakraborty, A. and Pai, L.-M. (2015). Regulation of CTP synthase filament formation during DNA endoreplication in Drosophila. *Genetics* **201**, 1511-1523. doi:10.1534/genetics.115.180737

Williams, J. C., Kizaki, H., Weber, G. and Morris, H. P. (1978). Increased CTP synthetase activity in cancer cells. *Nature* **271**, 71-73. doi:10.1038/271071a0

Wolfe, K., Kofuji, S., Yoshino, H., Sasaki, M., Okumura, K. and Sasaki, A. T. (2019). Dynamic compartmentalization of purine nucleotide metabolic enzymes at leading edge in highly motile renal cell carcinoma. *Biochem. Biophys. Res. Commun.* **516**, 50-56. doi:10.1016/j.bbrc.2019.05.190

Zhang, L., Luo, J., Wan, P., Wu, J., Laski, F. and Chen, J. (2011). Regulation of cofilin phosphorylation and asymmetry in collective cell migration during morphogenesis. *Development* **138**, 455-464. doi:10.1242/dev.046870

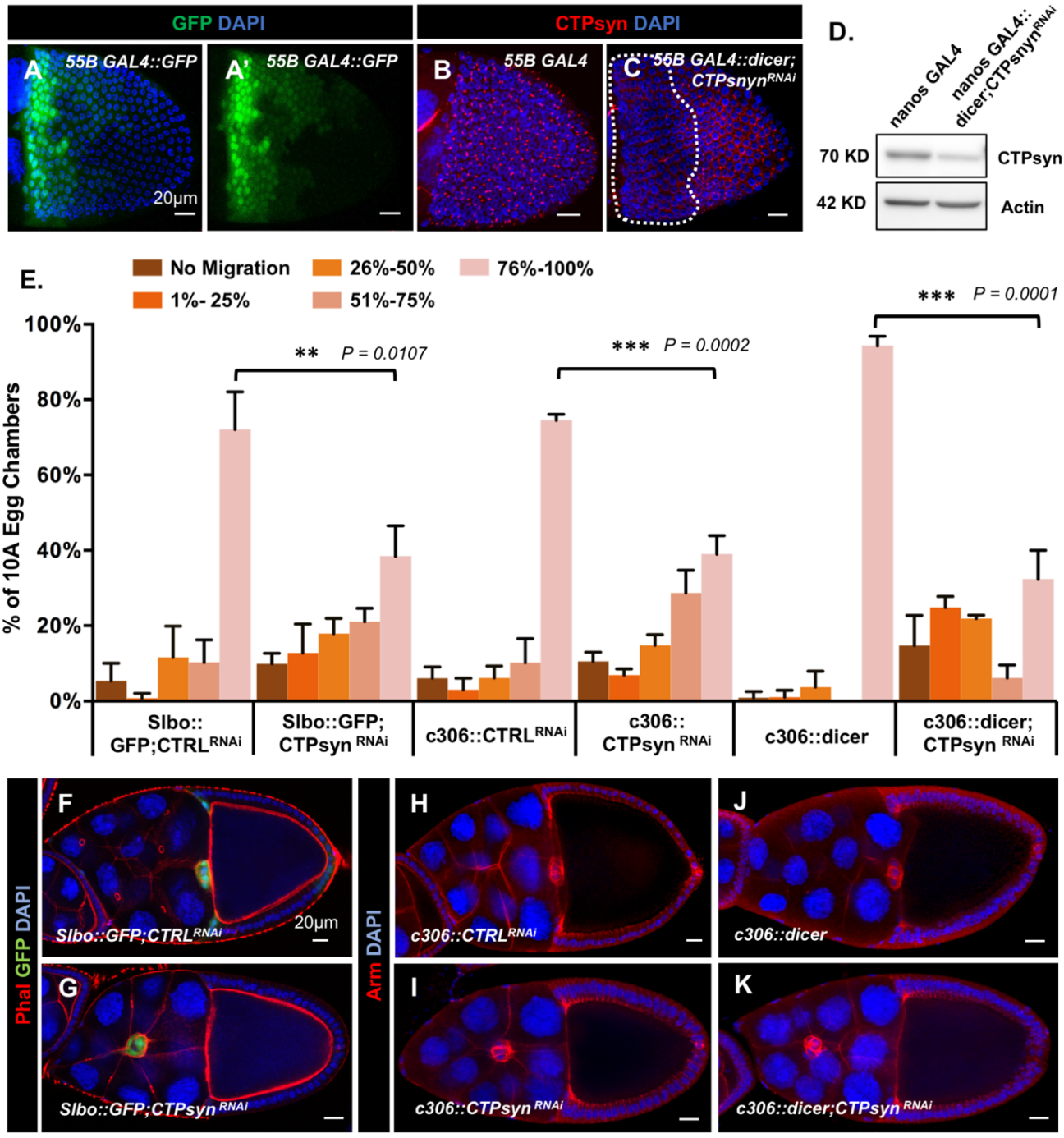

Fig. S1. Depletion of CTPsyn affected border cell migration

(A-A') Stage 10 egg chamber showing GFP expression in the anterior follicle cells when driven by *55B*-GAL4. The genotypes is *55B-GAL4::UAS-GFP/+*. **(B-C)** CTPsyn RNAi reduced CTPsyn filaments in anterior follicle cells (shown by dotted white line) when driven by 55B-GAL4. The genotype are *55B-*

GAL4 (as control, B) and *55B-GAL4::dicer/+;CTPsyn^{RNAi}/+* (C). Egg chambers are immunostained with CTPsyn antibody (red) and DAPI (blue). **(D)** Western blot image shows reduction of CTPsyn protein in *Drosophila* ovary when CTPsyn RNAi was driven by *nanos-GAL4*. The genotypes are *nanos-GAL4* (as control) *and nanos-GAL4::dicer/+; CTPsyn^{RNAi}/+*. **(E)** Quantification of border cell cluster migration delay in stage 10 egg chambers caused by RNAi mediated knockdown of CTPsyn, driven by *Slbo-Gal4* and *c306-Gal4*. The total egg chambers: 90<n<120. The averages come from three individual experiments. The results are shown as the mean ± SD; ***P <0.001 (two-tailed unpaired Student's t-test). **(F-K)** Representative images of the genotypes quantified in Fig. S1E. The genotypes are *Slbo-Gal4::CTRL^{RNAi}/+* (F), *Slbo-GAL4::CTPsyn^{RNAi}/+* (G), *c306-Gal4::CTRL^{RNAi}/+* (H), *c306-GAL4::CTPsyn^{RNAi}/+* (I), *c306-GAL4::dicer/+*(J), and *c306-GAL4::dicer/+;CTPsyn^{RNAi}/+* (K). Egg chambers are immunostained with Arm antibody (red) and DAPI (blue). All crosses were maintained at 29℃.

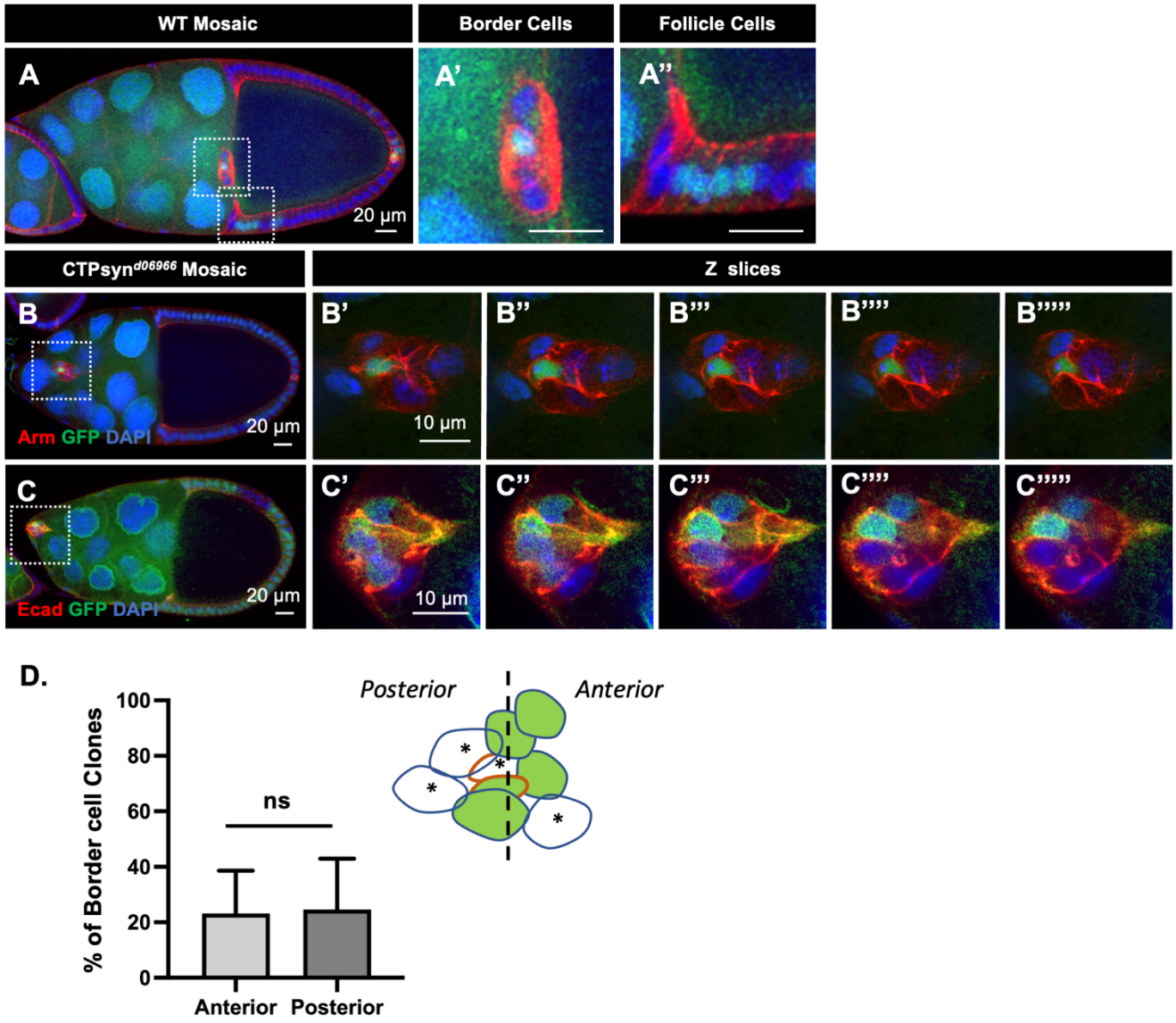

Fig. S2. Border cell cluster with CTPsyn mosaic mutant clones showed reduced migration

(A-C) Representative images of stage 10 egg chambers with Wild type (A) and CTPsyn mutant mosaic clones (B-C). Square box in Fig. A show enlarged view of Wild type mosaic clones in border cell cluster (A') and follicle cells (A''). Square box in Fig. B and C shows the enlarged view of the z-sections with CTPsyn mutant mosaic clones in border cell cluster (B'-B''''') (C'-C'''''). Egg chambers in Fig A and B are immunostained with Arm antibody (red) and DAPI (blue). Egg chamber in Fig. C is immunostained with Ecad antibody (red) and DAPI (blue). **(D)** Percentage of positional preference (anterior vs posterior) for the border cell clones were calculated for each border cell cluster (n=30). CTPsyn mutant clones were marked as GFP negative. The results are shown as the mean ± SD; n.s. (no significant) (two-tailed unpaired Student's t-test). The genotypes are *e22c-GAL4::UAS-FLP/+;Ubi-GFP, FRT80B /FRT80B* (A-A'') and *e22c-GAL4::UAS-FLP/+;Ubi-GFP, FRT80B /CTPsyn^{d06966} FRT80B* (B-D). Clones were induced at 29°C for 5 days.

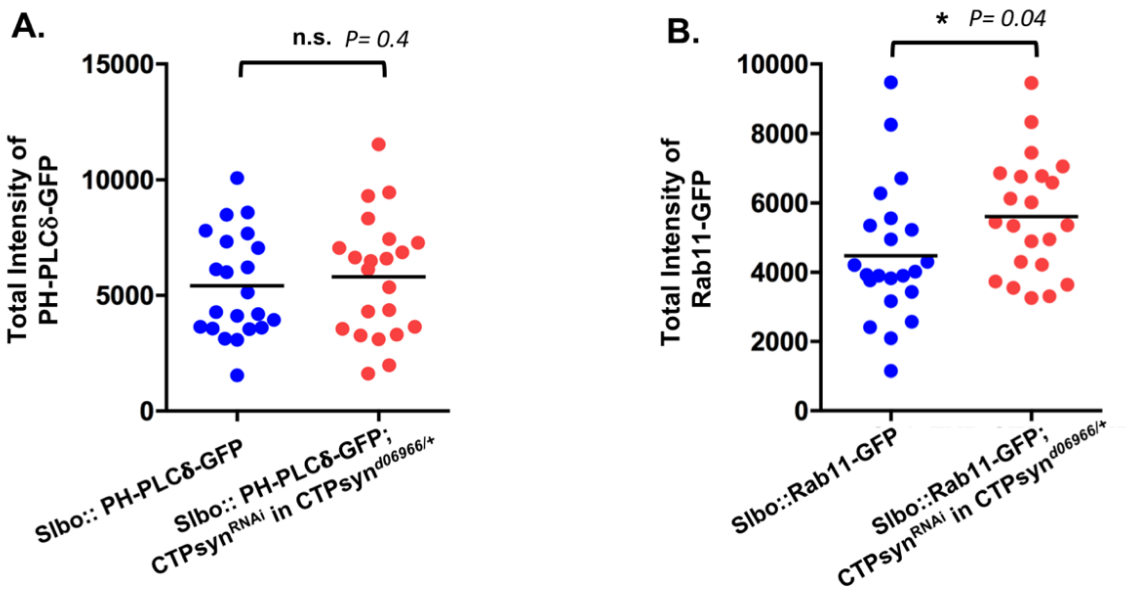

Fig. S3. Total PIP2 levels remains unaltered with CTPsyn depletion

(A) The total PIP_2 levels in control and CTPsyn-depleted border cells (n=22). **(B)** The total Rab11 level in control and CTPsyn-depleted border cell clusters (n=22). The results are shown as the mean ± SD; **P* <0.05 and n.s. (no significant) (two-tailed unpaired Student's t-test). All crosses were maintained at 29°C.

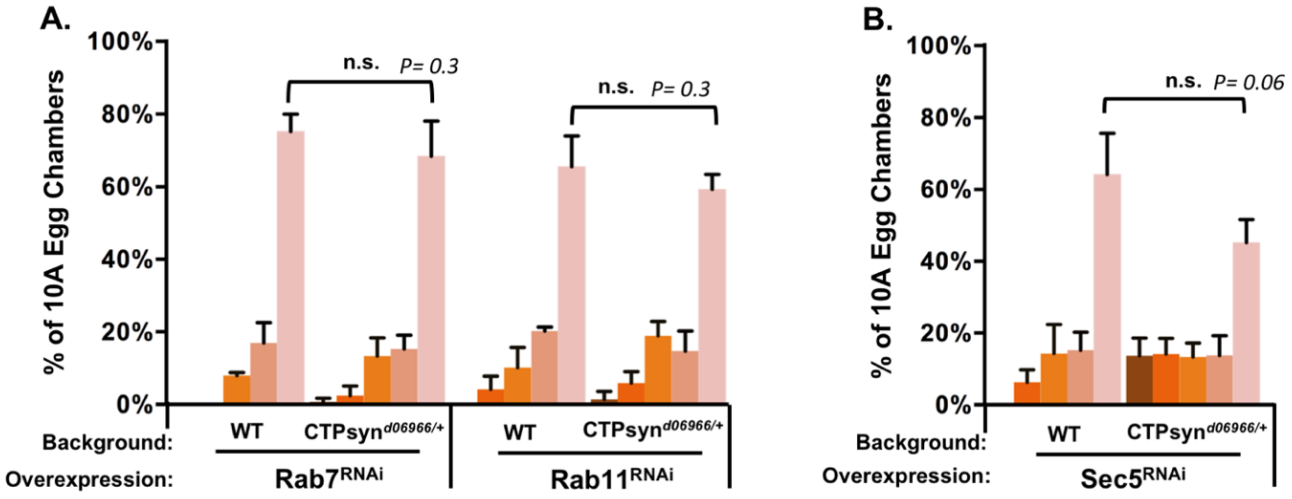

Fig S4. CTPsyn did not genetically interact with Rab11, Rab7 and Sec5 during collective cell migration.

(A-B) Rab7 and Rab11 (A) and Sec5 (B) knockdown in border cell clusters under *CTPsyn*^{d06966} heterozygous mutant background didn't affect border cell migration. The quantification of border cell migration average comes from three independent experiments. All crosses were maintained at 29°C. The total egg chambers in Fig S4A: 93<n<161. Fig S4A: 69<n<180. The results are shown as the mean ± SD; ***P <0.001 (two-tailed unpaired Student's t-test).

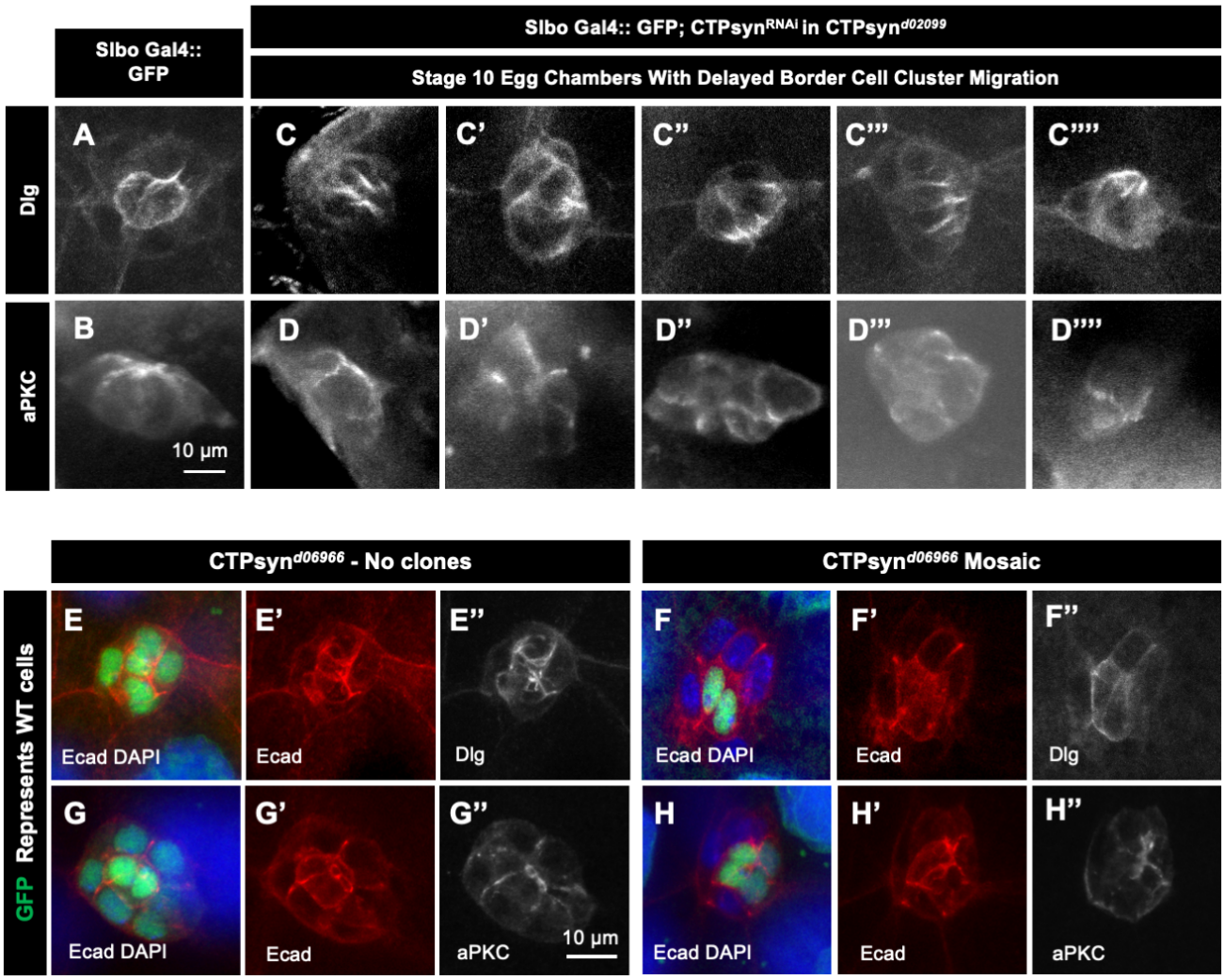

Fig. S5. Dlg and aPKC distributions were not affected in CTPsyn depleted border cell clusters

(A-B) The Dlg (A) and aPKC (B) patterns in control border cell cluster *(Slbo::UAS-GFP)*. **(C-D'''')** The Dlg (C-C'''') and aPKC (D-D'''') patterns in CTPsyn-depleted border cell clusters (*Slbo::UAS-GFP/+;UAS-CTPsyn^{RNAi}/ CTPsyn^{d06966}*). All crosses were maintained at 29℃. **(E-H")** The Ecad (E-E', G-G'), Dlg (E'') and aPKC (G'') staining of border cell clusters with no clones. The Ecad (F-F', H-H'), Dlg (F'') and aPKC (H'') staining of border cell clusters with *CTPsyn^{d06966}* mutant clones.

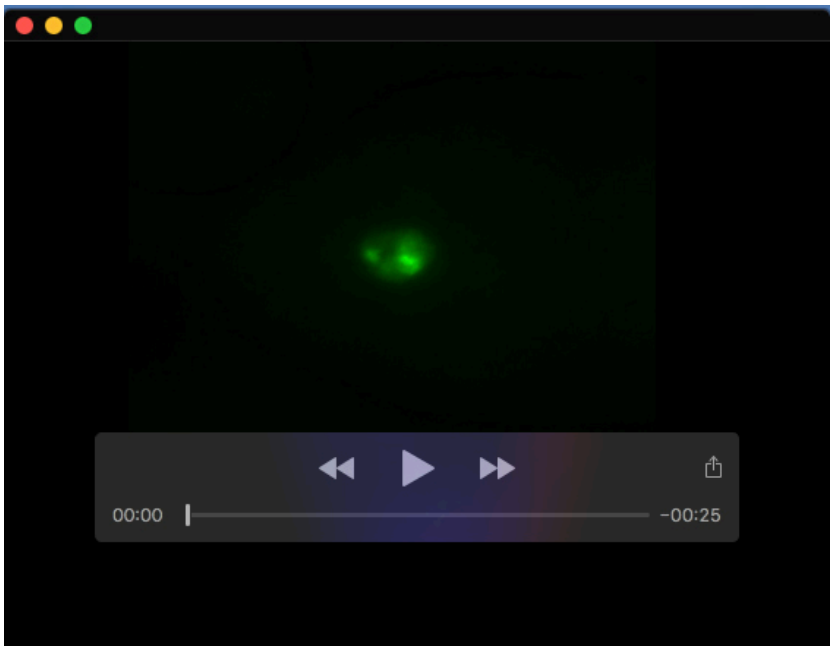

Movie 1. Control border cell cluster migration

Dynamic movement of control border cell cluster during migration. The images were acquired every 5 minutes for 94 frames and observed by a Zeiss Observer D1 microscope. Genotype is *hsFLP, UAS-mCD8-GFP/c306-Gal4;+; FRT80B/ tubGAL80 FRT80B.*

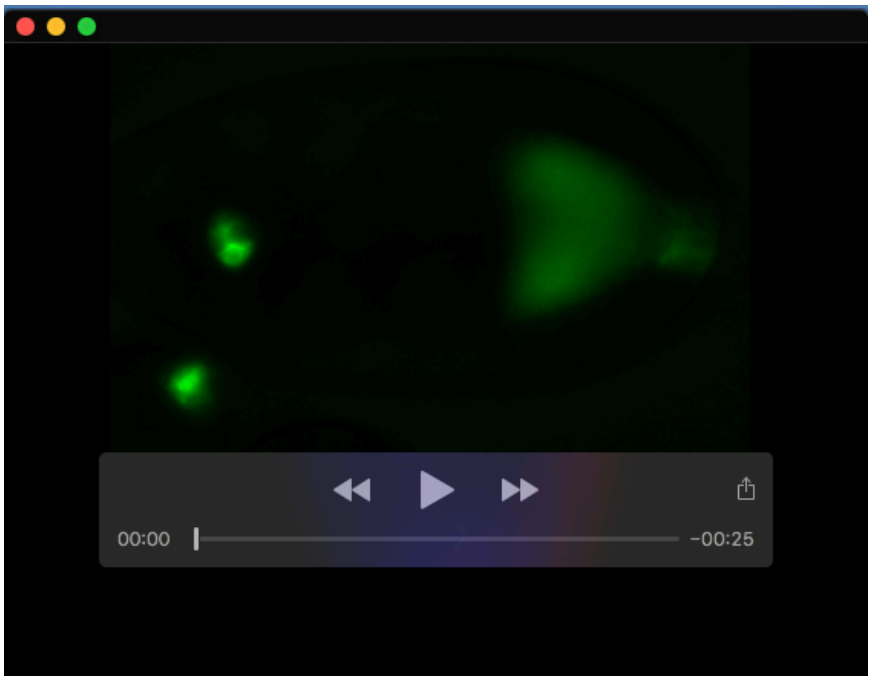

Movie 2. CTPsyn mutant border cell cluster migration

CTPsyn mutant border cell cluster showed impaired rotation during migration. The images were acquired every 5 minutes for 104 frames and observed by a by Zeiss Observer D1 microscope. Genotype is *hsFLP, UAS-mCD8-GFP/c306-Gal4;+;CTPsyn*^{d06966}*FRT80B/ tubGAL80 FRT80B*.